THE AMERICAN SOCIETY OF MECHANICAL ENGINEERS
345 E. 47 St., New York, N.Y. 10017

92-GT-201

An Experimental Study of Film Cooling in a Rotating Transonic Turbine

REZA S. ABHARI
Textron Lycoming
Stratford, CT 06497

A. H. EPSTEIN
Massachusetts Institute of Technology
Cambridge, MA 02139

ABSTRACT

Time-resolved measurements of heat transfer on a fully cooled transonic turbine stage have been taken in a short duration turbine test facility which simulates full engine non-dimensional conditions. The time average of this data is compared to uncooled rotor data and cooled linear cascade measurements made on the same profile. The film cooling reduces the time-averaged heat transfer compared to the uncooled rotor on the blade suction surface by as much as 60%, but has relatively little effect on the pressure surface. The suction surface rotor heat transfer is lower than that measured in the cascade. The results are similar over the central 3/4 of the span implying that the flow here is mainly two-dimensional. The film cooling is shown to be much less effective at high blowing ratios than at low ones. Time-resolved measurements reveal that the cooling, when effective, both reduced the d.c. level of heat transfer and changed the shape of the unsteady waveform. Unsteady blowing is shown to be a principal driver of film cooling fluctuations, and a linear model is shown to do a good job in predicting the unsteady heat transfer. The unsteadiness results in a 12% decrease in heat transfer on the suction surface and a 5% increase on the pressure surface.

NOMENCLATURE

$A(\omega)$	Fourier coefficient at frequency (ω)
d	equivalent slot width
$f(x)$	function of length
$G(\omega)$	damping coefficient
h	heat transfer coefficient
L	length of coolant slot
M	Mach number
Nu	Nusselt number based on axial chord, inlet total temperature, wall temperature, and main gas conductivity at the wall
Pr	Prandtl number
Q	heat flux
Re_c	Reynolds number based on axial chord, isentropic exit Mach number, and properties at exit condition
S	surface length downstream of coolant holes
t	time
T	temperature
U	velocity
x	length scale
α	coolant injection angle relative to surface normal
ϕ	perturbation potential
η	effectiveness
κ	modified reduced frequency
μ	viscosity
ρ	density
θ	non-dimensional coolant temperature
Ω	reduced frequency
ω	oscillation frequency
ξ,β	non-dimensional blowing parameters

Subscripts

0	uncooled
ad	adiabatic
aw	adiabatic wall
c	coolant
fc	film cooled
x,t	derivative with respect to x or t
∞	freestream conditions

Superscripts

$()'$	perturbation quantity
$\overline{()}$	time-averaged condition

INTRODUCTION

The accurate prediction of film cooling on turbine profiles and the end-walls is a major factor in the continuing effort to increase turbine entry temperature. The designer's goal is to use the minimum amount of coolant necessary to insure adequate turbine life. To this end, there has been considerable research over the past 30 years to increase our understanding of coolant film behavior and its interaction with the freestream flow. Film-cooled boundary layer behavior has been shown to be quite complex with wall curvature, three-dimensional external flow structure, free-stream turbulence, compressibility, and unsteadiness, all influencing cooling performance.

Many studies have focused on film cooling in simple geometries, on two-dimensional flat and curved plates in steady flow. For example, Ito et al. (1978) showed that the blade surface curvature influences the film cooling effectiveness particularly in the vicinity of

Presented at the International Gas Turbine and Aeroengine Congress and Exposition
Cologne, Germany June 1-4, 1992
This paper has been accepted for publication in the Transactions of the ASME
Discussion of it will be accepted at ASME Headquarters until September 30, 1992

the injection holes, with greater effectiveness on the convex surface and less on the concave surface, as compared to a flat plate case. On the concave surface, Schwarz and Goldstein (1988) suggested that the unstable flow along the concave surface promotes lateral mixing of the film cooling jets, which in turn results in a two-dimensional behavior of the film effectiveness.

More recently, studies of the steady flow in linear cascades has provided detailed measurements of film cooling performance on three-dimensional blade surfaces. Near the endwalls on the suction surface of the blade profile, Goldstein and Chen(1985) showed that the film cooling jets are swept away from the surface by the passage vortex, resulting in low levels of film effectiveness. On the concave surface, the film cooling was unaffected by endwall influences.

Relatively less work has been done in the unsteady rotating environment characteristic of a rotor blade. Dring et al (1980) studied the performance of film cooling in a low speed rotating facility. They observed a large radial displacement of the coolant jet on the pressure surface, which they concluded to be the main cause of the low level of effectiveness measured. Recently, Takeishi et al. (1991) reported measurements of film effectiveness on a rotating turbine stage. The overall conclusion of both studies was that on the rotor midspan, the suction surface film cooling effectiveness is similar to existing flat plate and cascade measurements, while on the pressure surface, a much higher decay rate of effectiveness was measured.

The influence of the NGV trailing edge slot coolant ejection on the downstream rotor time-averaged heat transfer was reported by Dunn (1986), who observed that NGV injection increased heat transfer on the downstream rotor by as much as 20%. Dunn's data also showed little effect on the heat transfer as the coolant to freestream gas temperature was raised from 0.52 to 0.82.

The intent of the present study is to experimentally quantify the influence of three-dimensional and unsteady effects on the rotor film cooling process in a transonic rotating turbine stage. The approach is to measure the steady and time resolved chordwise heat flux distribution at three spanwise locations in a fully scaled short duration turbine rig. Here, we examine both the mean and time resolved heat transfer with film cooling and compare those results to measurements from an uncooled turbine with the same geometry and with cooled cascade data. An unsteady numerical calculation and analytical modelling is then used to elucidate the time resolved fluid mechanics in the turbine rotor. Finally, the average heat transfer results are explained in terms of the time resolved details.

TABLE 1
MIT BLOWDOWN TURBINE SCALING

	Full Scale	MIT Blowdown
Fluid	Air	Ar-Fr 12
Ratio specific heats	1.28	1.28
Mean metal temperature	1118°K (1550°F)	295°K (72°F)
Metal/gas temp. ratio	0.63	0.63
Inlet total temperature	1780°K (2750°F)	478°K (400°F)
True NGV chord	8.0 cm	5.9 cm
Reynolds number*	2.7×10^6	2.7×10^6
Inlet pressure, atm	19.6	4.3
Outlet pressure, atm	4.5	1.0
Outlet total temperature	1280°K (1844°F)	343°K (160°F)
Prandtl number	0.752	0.755
Eckert number†	1.0	1.0
Rotor speed, rpm	12,734	6,190
Mass flow, kg/sec	49.0	16.6
Power, watts	24,880,000	1,078,000
Test time	Continuous	0.3 sec

* Based on NGV chord and isentropic exit conditions
† $(\gamma\text{-}1)M^2T/\Delta T$

EXPERIMENTAL APPARATUS

These experiments were conducted in a short duration (0.3 sec) blowdown turbine test facility at MIT which simulates full engine scale Reynolds number, Mach number, Prandtl number, gas to wall and coolant to mainstream temperature ratios, specific heat ratios, and flow geometry (Table 1) (Epstein et al., 1986). The corrected speed and weight flow where kept constant to better than 0.5% over the test time. The turbulent intensity at the nozzle guide vane inlet was less than 1%.

For the tests reported herein, a coolant injection system was added to the facility. The coolant system consisted of a refrigerated coolant supply tank (200°K minimum), metering orifice, and fast-acting (15 ms) shutoff valve. The flow path from the coolant tank to the NGV's and rotor spin-up nozzles was internally insulated with teflon and syntactic foam epoxy to reduce heat transfer. The coolant tank and metering orifice were sized such that the time rate of change of pressure in the coolant tank matched that of the main flow supply tank. Thus, the coolant to main flow mass flux ratio (the blowing ratio) remains constant (±2%) over the test time. An argon/freon gas mixture was used for the coolant in order to match the ratio of specific heats of engine coolant (1.36). Freon-14 was selected (as opposed to freon-12 in the main flow) to prevent condensation at the low temperatures and high pressures of the coolant supply system.

High frequency response pressure transducers and thermocouples were installed in the NGV's and rotor blades to monitor the conditions in the coolant hole supply plenums. All worked well except for the rotor thermocouples which were unreliable. Facility measurements for these tests included inlet total temperature and pressure, outlet total pressure, wall static pressures, and rotor speed.

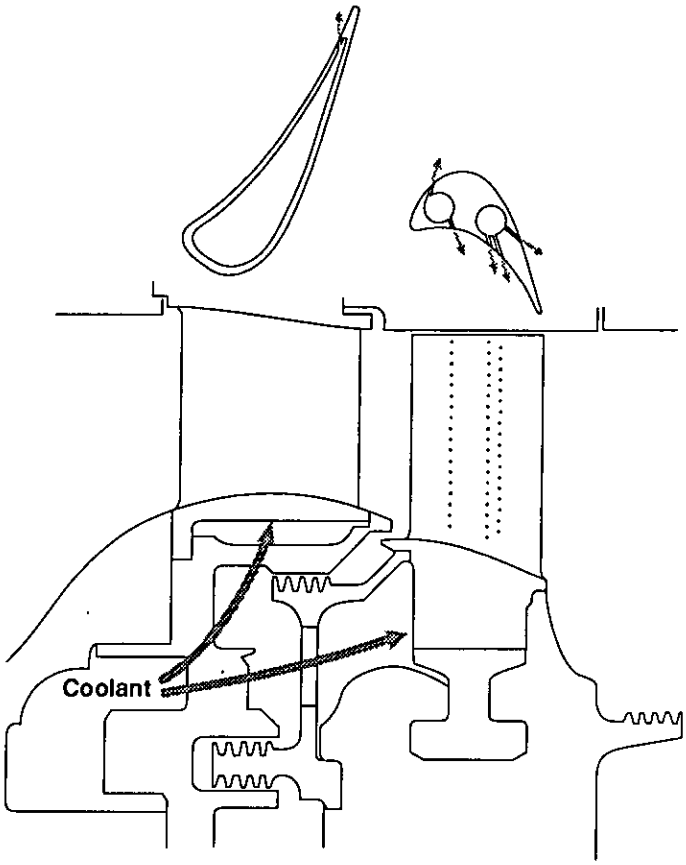

Fig. 1: Turbine geometry and cooling arrangement

TABLE 2
TURBINE DESIGN PARAMETERS

Turbine loading, $\Delta H/U^2$	-2.3
Total pressure ratio	4.2
Velocity ratio, C_x/U	0.63
Rotor aspect ratio	1.5
NGV exit Mach No.	1.18
Rotor coolant/Main flow	6%
NGV Coolant/Main flow	3%

Of interest here is the measurement of the time-resolved heat flux distribution about the rotor blade. The thermal inertia of the blades is such as to keep the blade wall temperature essentially constant during the test at the pretest initial temperature (room temperature). Thus, uncooled rotor blading behaves as though it were internally cooled, generating a heat flux from the free stream into the blade. This flux is measured with thin film heat flux gauges distributed about the blade profile. These transducers are 25 μm thick with a rectangular sensing area (1.0 x 1.3 mm), oriented such that the longer dimension is in the chordwise direction. The frequency response of these instruments extends from d.c. to 100 kHz. The gauges are individually calibrated and relative gauge calibrations are accurate to better than 5%. Absolute calibration accuracy is about 10%. Uncertainty was evaluated for each transducer and is noted in the subsequent figures. Details of the gauge theory, data reduction, and calibration may be found in Epstein et al. (1986). For the data presented herein, the signals from the heat flux gauges were digitized at a 200 kHz sampling rate (33 times blade passing). Unless otherwise specified, the digital signal was then ensemble-averaged for 360 vane passing periods (Guenette et al., 1989). Nusselt numbers are defined in terms of rotor relative frame mass averaged NGV exit temperature, the measured surface temperature, the gas thermal conductivity at that temperature, and the rotor axial chord.

The 0.5 meter diameter turbine tested (Fig. 1) was a single-stage, 4:1 pressure ratio transonic machine whose design parameters are given in Table 2 (Rigby et al., 1990). This turbine geometry has been extensively studied in cooled and uncooled cascades (Ashworth et al., 1987) and as an uncooled stage (Abhari et al., 1991). For these tests of cooled rotor heat transfer, thin walled nozzle guide vanes (NGV's) were used with slot injection near the pressure surface trailing edge sized to pass the flow of a fully cooled NGV. Solid rotor blading was used for the uncooled tests. For the cooled testing, the solid aluminum blades were drilled out for two coolant supply plenums. The film coolant hole configuration was chosen to provide the maximum information on coolant performance in rotating geometries rather than be representative of a production blade cooling configuration. The coolant hole internal diameters (0.5 mm) were 2% of axial chord. All rows had circular exit areas except for the first row on the suction surface which was D-shaped. The coolant hole and heat flux gauge locations are shown in Fig. 2. The top chordwise row will be referred to as the tip location, the middle as midspan, and the bottom as the hub gauges. These locations were chosen so as to elucidate the spanwise variation in the flow insofar as possible without intruding into the endwall flow region (Norton, 1987). Unfortunately, several of the gauges failed over the course of the testing (especially on the pressure surfaces), so not all measurement locations yielded data at all test conditions. All data taken during each test are reported.

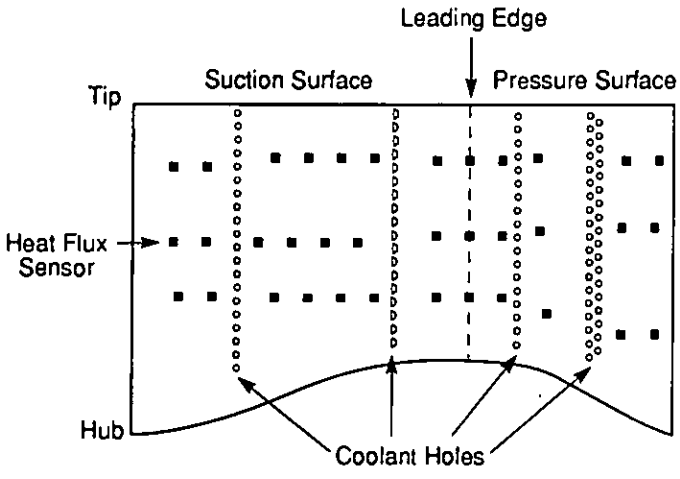

Fig. 2: Composite of the heat flux gauge and coolant hole positions on the projected blade surface. Note that each of the three chordwise rows of gauges is on a separate blade.

STEADY STATE MEASUREMENTS

As a prelude to measurements of the fully cooled stage, the uncooled rotor was tested behind cooled nozzle guide vanes. This was done to permit differentiation of the influence of the cold nozzle guide vane wakes (cold streaks to the rotor) from the effects of fully cooling the stage. (A cooled rotor behind uncooled NGV's may also be informative but was not done due to time constraints.) Figure 3 compares the steady state heat transfer distribution about the uncooled rotor midspan behind both cooled and uncooled NGV's. (The chordwise sensor placement on the uncooled blade differs somewhat from the cooled blade placement illustrated in Fig. 2. The uncertainty in the measurements is indicated by a vertical bar unless it is less than the symbol size.) The coolant injection is 3.0% of the main mass flow rate and the coolant to free stream temperature ratio is 0.63. The heat transfer at the leading edge drops by 18% with injection while the pressure surface heat transfer increases monotonically from the leading edge. Relatively little change is observed on the suction surface. Examination of the time-resolved data showed that the waveform shapes on the pressure surface were no different with and without injection, that only the d.c. levels changed. Tests run at different rotor speeds and blowing ratios showed similar results. At this time, we are uncertain as to the physical origin of these observed effects – changes in the NGV shock pattern due to the mass injection,

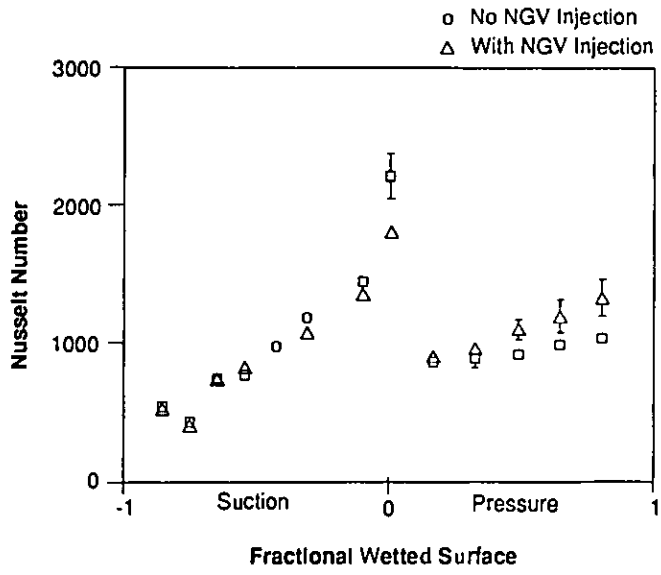

Fig. 3: Influence of nozzle guide vane trailing edge injection on uncooled rotor heat transfer

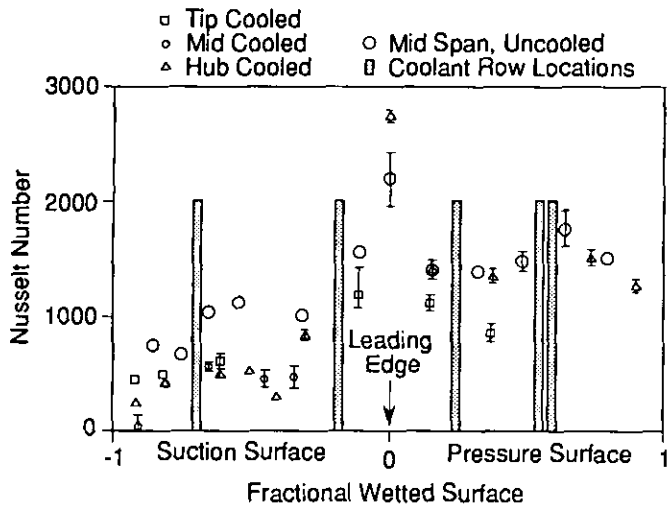

Fig. 4: Time-averaged heat transfer of fully cooled stage compared to that of the same profiles as an uncooled stage at -10° rotor incidence and 120% of design Reynolds number

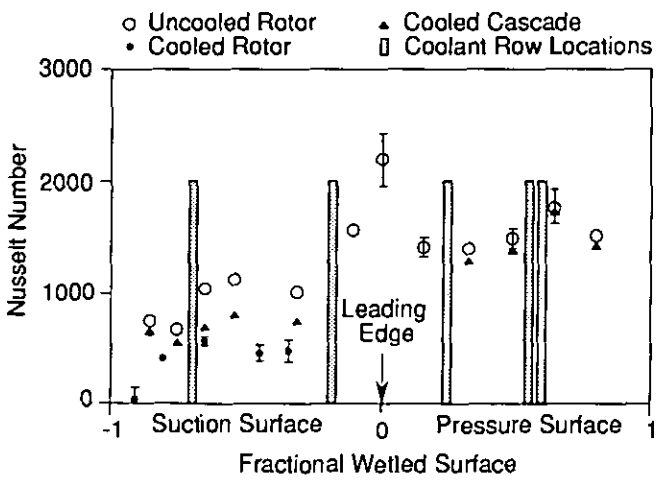

Fig. 6: Uncooled and film cooled rotating stage measurements compared with those from a cooled linear cascade

increased NGV wake turbulence and velocity deflect, or changed wake temperature are all possible candidates. Work is currenly underway to explain them in a quantitative fashion.

Measurements made on the fully cooled stage are shown in Fig. 4, along with earlier uncooled stage results taken at the same operating condition (-10° rotor incidence, 120% of the baseline Reynolds number). The shaded bars denote the location of the rows of coolant injection holes. Figure 5 presents the data of Fig. 4 along with that from a second test taken two months later to check repeatability. The results from the two tests are very similar with the exception of one tip section gauge on the pressure and suction surfaces. It can be seen from the data in these plots that the suction and pressure surfaces behave quite differently. The film cooling is effective on the suction surface in reducing the blade heat transfer with similar results observed across the span, implying that the flow here is somewhat two-dimensional. By comparison, little reduction in heat transfer is observed along the pressure surface except near the tip.

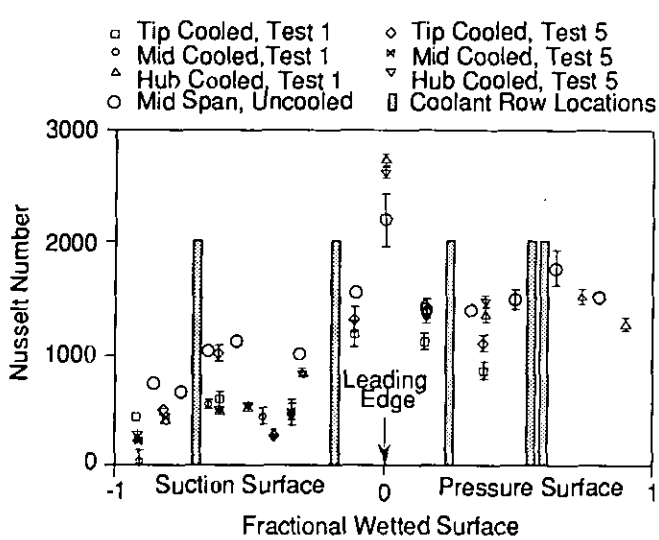

Fig. 5: Comparison of data from two tests illustrating level of measurement repeatability

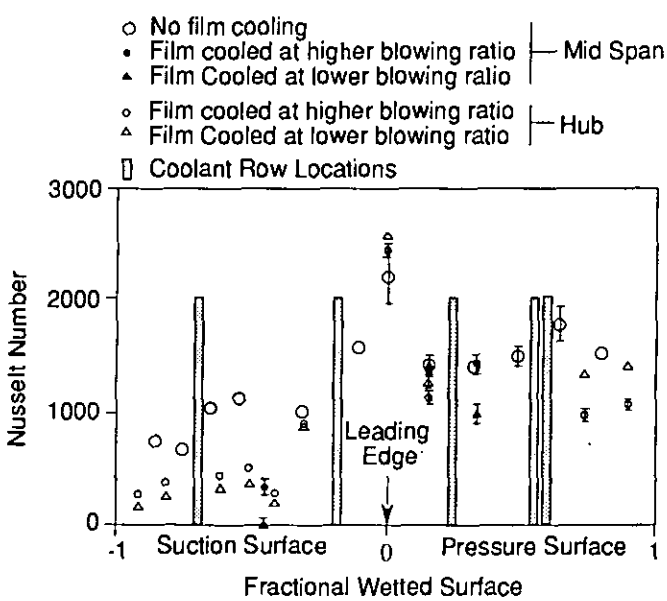

Fig. 7: The influence of blowing ratio on rotor heat transfer

TABLE 3
COOLANT TEST CONDITIONS

Temperature Ratios	
NGV Coolant/Freestream	0.54
Rotor Coolant/Freestream Relative	0.51
Rotor Coolant/Wall	0.74
Momentum Ratios, 1st Row of Holes	
Suction Surface	0.72
Pressure Surface	1.10
Blowing Ratios, 1st Row of Holes	
Suction Surface, High/Low	1.24/0.96
Pressure Surface, High/Low	1.52/1.1

Rigby et al. (1990) performed measurements on the same cooled profile in a linear cascade. Figure 6 compares the cascade measurements with those from the rotating stage with both a cooled and uncooled rotor. The data show that heat transfer is reduced on the suction surface of the rotor compared to the cascade, by as much as 60%. On the pressure surface, the cooled cascade data show little influence of film cooling.

The influence of blowing ratio (coolant mass flow/freestream mass flow) on film cooling was examined by replacing the usual Argon-Freon 14 coolant with nitrogen, changing the coolant molecular weight and ratio of specific heats, thus reducing the blowing ratio without appreciably changing the momentum ratio (momentum of coolant flow/momentum of freestream flow), Table 3. Although somewhat sparse, the data in Fig. 7 show that, on the suction surface, reducing the blowing ratio reduces the heat transfer. The data on the pressure surface are less uniform, with lowered blowing ratio reducing the heat transfer downstream of the first row of holes, but downstream of the second row, the heat transfer is reduced at the higher blowing ratio. This behavior would be consistent with film lift-off at the higher blowing ratios.

Overall, we note that the film cooling appears effective on the rotor suction surface but much less so on the pressure surface. The lack of more detailed spatial coverage (due to instrumentation failures) inhibits more detailed conclusions from the steady state data. With the exception of Fig. 7, all the data in this paper was taken at the higher blowing ratio, corresponding to the design intent.

TIME-RESOLVED MEASUREMENTS

Time-resolved data are compared with uncooled rotor measurements in Fig. 8. Over the pressure surface, there is little or no reduction in heat transfer from the film cooling. On the suction surface, the influence of film cooling is more pronounced. At the crown of the suction surface (Fig. 8a), the cooling is pronounced at midspan but minimal at the hub. Elsewhere along the suction surface, the cooling is similar at hub and midspan. The influence of the film cooling is seen to both reduce the heat transfer and also to introduce a phase shift in the unsteady waveform.

The influence of blowing ratio on the pressure surface (position corresponding to Fig. 8i) is illustrated in Fig. 9. At the higher blowing ratio, the film provides no cooling at all while at the lower blowing ratio, the mean heat transfer is reduced by about 30% and the waveform is altered.

The fractional change in heat transfer (the isothermal film effectiveness) calculated from the midspan data on the crown of the suction surface (Fig. 8a) is shown in Fig. 10. Note that for about half of a vane passing period, the effectiveness is approximately constant at 0.7, but then drops rapidly to zero. In the following section, we examine the nature of this unsteadiness and present a simple time-resolved model of the process.

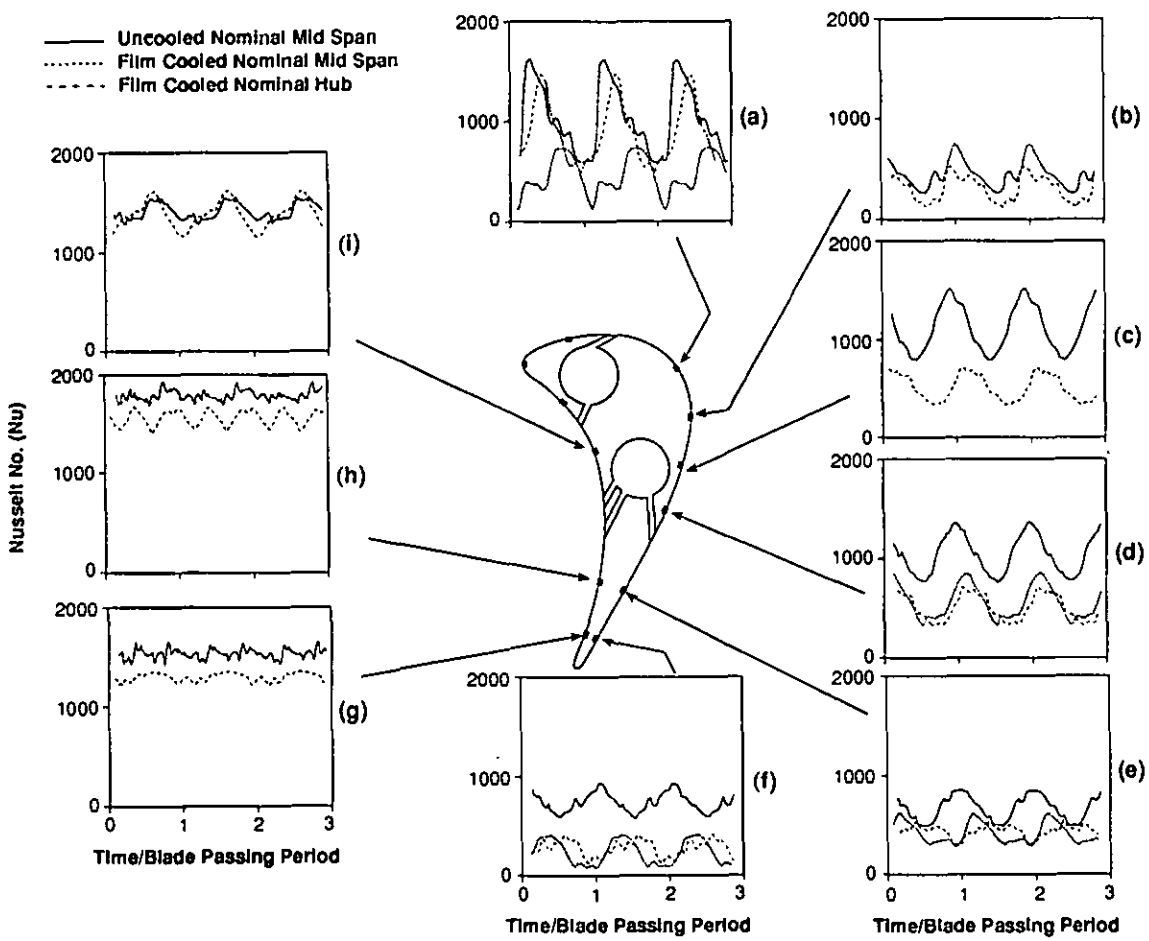

Fig. 8: Time-resolved rotor heat transfer measurements compared with those for an uncooled rotor

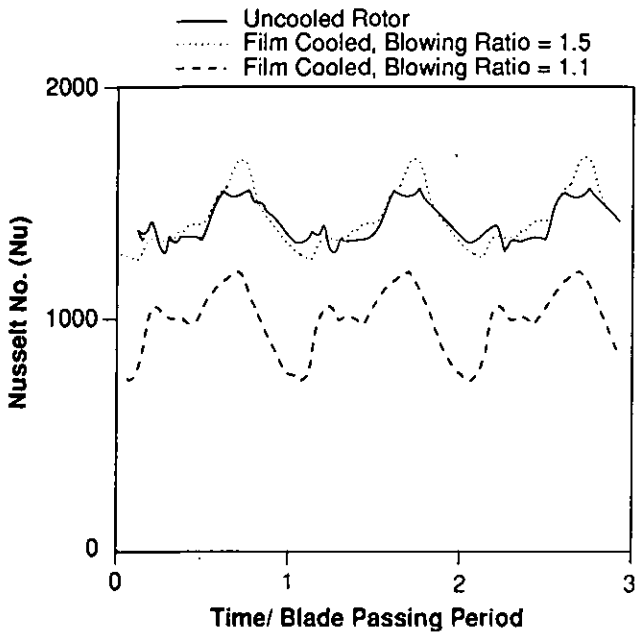

Fig. 9: The influence of blowing ratio of the upstream coolant hole on the pressure surface heat transfer corresponding to Fig. 8 (i)

THE INFLUENCE OF UNSTEADINESS ON ROTOR FILM COOLING

Turbine blade aerodynamic and cooling design is currently based on the assumption that the flow can be modelled as steady. The data presented here certainly show that blade heat transfer is unsteady over much of the airfoil surface. What are the sources of these fluctuations, which are dominant, how can they be modelled, and what are the turbine design implications of this unsteadiness?

There are many sources of unsteadiness in turbine rotors. Potential interactions between blade rows and impingement of NGV wakes and shock waves on the rotor are the predominant sources of free stream unsteadiness. Abhari et al. (1991) showed that a two-dimensional, unsteady, multi-blade row, viscous code (UNSFLO, Giles and Haimes, 1991) can quantitatively predict the time-resolved heat transfer in an uncooled configuration of this turbine stage.

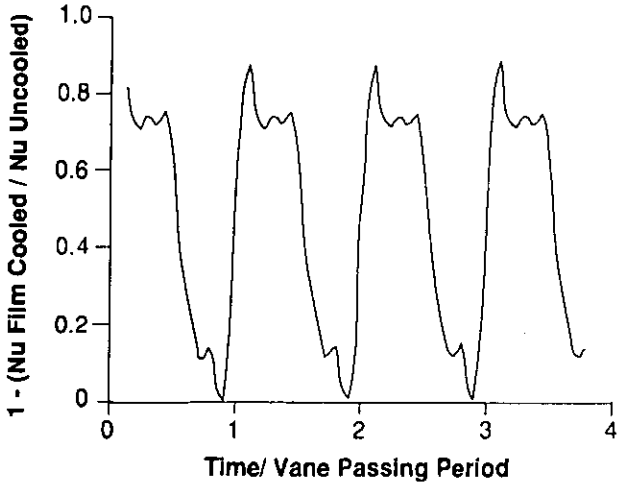

Fig. 10: Time-resolved isothermal effectiveness calculated from the midspan data on the crown of the rotor suction surface (Fig. 8 (a))

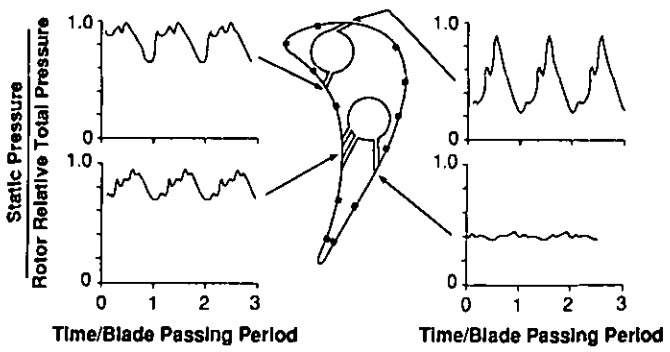

Fig. 11: Time-resolved wall static pressure at the coolant hole exit locations as predicted by an unsteady, multi-blade row code

The flow and heat transfer perturbations in a transonic turbine are large, of the order of the mean flow. Figure 11 presents the static pressure history calculated with the unsteady code for the uncooled turbine at the locations corresponding to the injection holes on the cooled rotor. This shows large fluctuations, especially near the front of the blade. The unsteady envelope of the rotor static pressure distribution is compared with the coolant supply plenum pressure in Fig. 12 and shows that the coolant driving pressure ratio can vary enormously, by more than 100% over some of the blade chord. Although in the time mean, the coolant minus wall static pressure difference is always positive, the instantaneous pressure difference is zero near the rotor leading edge over part of the vane passing period. On the suction surface, the variation in coolant driving pressure difference is sufficient to choke the coolant holes during part of the cycle and reverse the flow during another part! For this temporal pressure variation to influence the mass flow rate of coolant, the vane passing frequency must be low compared with the propagation time of disturbances through the coolant holes. For this turbine, the product of coolant mean flow Mach number and reduced frequency ($\Omega = \omega L/U_c$) is 0.4, implying that pressure perturbations will indeed modify the coolant flow rate.

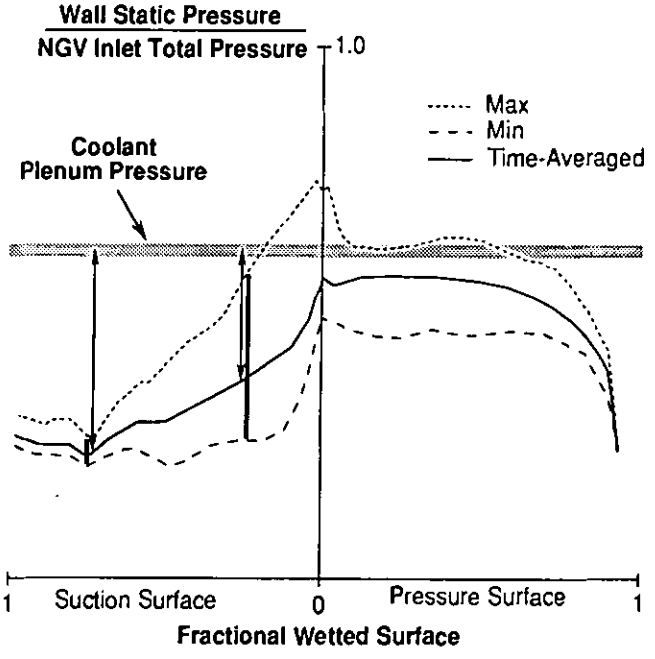

Fig. 12: Midspan rotor static pressure distribution as predicted by an unsteady, multi-blade row, viscous code

To model this process, we will formulate a simple unsteady, one-dimensional, subsonic compressible flow through a slot and drive it with the pressure perturbations calculated by the time-resolved multi-blade row code. Linearized about the mean flow, the potential perturbation satisfies (Ashley and Landahl, 1965)

$$U = \overline{U} + U' = \overline{U}\left[1 + \frac{\partial \varphi(x,t)}{\partial x} + \ldots\right] \tag{1}$$

and

$$\left(1 - \overline{M}^2\right)\varphi_{xx} - \frac{2\overline{M}^2}{\overline{U}}\varphi_{xt} - \frac{\overline{M}^2}{\overline{U}^2}\varphi_{tt} = 0 \tag{2}$$

Assuming a harmonic unsteady perturbation of the form $\varphi = f(x)e^{i\omega t}$, the above linear partial differential equation reduces to a linear ordinary differential equation, the solution of which provides the mean unsteady mass flux from the holes. Summing for all frequencies and ignoring the second order terms (terms involving the square of the perturbation), the correction to the mean mass flow from the slot is given by

$$\overline{(\rho U)} = \overline{(\overline{\rho} + \rho')(\overline{U} + U')} = \overline{\rho U} + \overline{(\rho' U')} \approx \overline{\rho U}, \tag{3}$$

$$\text{when } \overline{(\rho' U')} << \overline{\rho U}$$

where ρ is the coolant density, U is the velocity, overbar corresponds to mean conditions, and prime corresponds to the perturbation quantities. At the exit of the coolant holes, the unsteady mass flux from the coolant slot including the first order correction, is written as

$$\frac{\rho U}{\overline{\rho U}} = \frac{\overline{\rho U} + (\rho U)'}{\overline{\rho U}} \approx \sum_{\omega=\omega_1}^{\infty} \left(1 - A(\omega)\, G(\omega)\, e^{i\omega t}\right) \tag{4}$$

where

$$G(\omega) = 1 - \overline{M}\frac{(1-\overline{M})e^{-i\kappa} + (1+\overline{M})e^{i\kappa}}{(1-\overline{M})e^{-i\kappa} - (1+\overline{M})e^{i\kappa}}, \quad \text{and} \quad \kappa = \frac{\overline{M}\,\Omega}{1-\overline{M}^2}$$

The term $A(\omega)$ is the Fourier coefficients of the periodic pressure at the exit of the coolant holes. Ω is the reduced frequency ($\omega L/U_c$) based on the slot length (L), and the mean coolant velocity (U_c). It is seen that as $\omega \rightarrow 0$, the term $G(\omega)$ also approaches zero and the quasi steady conditions are recovered. For a Mach number of 0.8 and a reduced frequency of 0.4, Eq. (4) indicates that the fluctuation in the coolant mass flux through the slot is 30%.

Given that the mass flux from coolant holes is unsteady, the film cooling must be unsteady as well. Whitten et al. (1970) have shown that, in a turbulent boundary layer with non-uniform blowing, film cooling is influenced principally by the local boundary layer conditions and shows little effect of prior history. This suggests that, at distances relatively close to the cooling holes compared to the chord, film cooling with unsteady blowing may behave as if the local flow were quasi-steady. To test this assumption, we will use a steady state film cooling correlation from the literature and drive it with the unsteady blowing as described in Eq. (4), using the unsteady, multi-blade row calculation to supply the wall static pressure at coolant hole locations. The estimated cooling effectiveness will then be used to "correct" the heat flux measured about the uncooled rotor in order to predict the cooled blade heat transfer. For this purpose, we employ the film cooling correlation suggested by Goldstein and Haji-Sheik (1967) for the adiabatic cooling effectiveness.

$$\eta_{ad} \equiv (T_\infty - T_{ad}) \,/\, (T_\infty - T_c) \tag{5}$$

$$\eta_{ad} = 5.75\, Pr^{2/3}\, \xi^{-0.8}\left(Re_c \frac{\mu_c}{\mu_\infty}\right)^{0.2} \beta^{-1} \tag{6}$$

Where

$$\beta \equiv 1 + \left(1.5 \times 10^{-4} \cos\alpha\; Re_c \frac{\mu_c}{\mu_\infty}\right)$$

$$\xi \equiv \left(\frac{S}{d}\right)\frac{(\rho U)_\infty}{(\rho U)_c}$$

α is the injection angle, Re_c is the Reynolds number based on the coolant fluid through the slot (Fig. 13). In this model, the coolant hole is a slot, so d represents an equivalent slot width defined as the hole area divided by the pitch between holes (Goldstein et al., 1974). It is assumed that the correction to the driving temperature due the compressibility is negligible. The time lag required for the coolant fluid to reach any point S, is assumed to be 70% of the freestream velocity, which corresponds to the mean propagation velocity of a turbulent patch within the boundary layer, as measured by Ashworth (1987).

Then, the ratio of heat transfer with film cooling ($\dot{Q}_{fc}$) to that without ($\dot{Q}_0$) is

$$\frac{\dot{Q}_{fc}}{\dot{Q}_0} = \frac{h_{fc}}{h_0}\left(\frac{T_{ad} - T_w}{T_\infty - T_w}\right) = \frac{h_{fc}}{h_0}\left(1 - \theta\,\eta_{ad}\right) \tag{7}$$

$$\theta \equiv \left(\frac{T_\infty - T_c}{T_\infty - T_w}\right)$$

Assuming that the heat transfer coefficient is unchanged by the addition of the coolant, then Eq. (7) can be written in non-dimensional form as

$$Nu_{\text{film cooled}}(S,t) \approx Nu_{\text{uncooled}}(S,t)\left(1 - \theta\,\eta_{ad}(S,t)\right) \tag{8}$$

We can now evaluate Eq. (8) using the uncooled rotor measurements to provide Nu_{uncooled} (S,t) and the unsteady, multi-blade row calculation to provide the time history of the wall static pressure (i.e. the calculations in Fig. 11) needed to estimate the unsteady blowing rate.

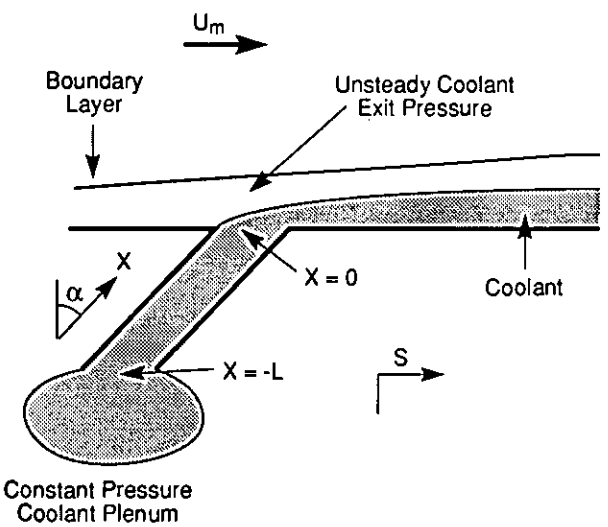

Fig. 13: Two-dimensional coolant slot model with unsteady external pressure field

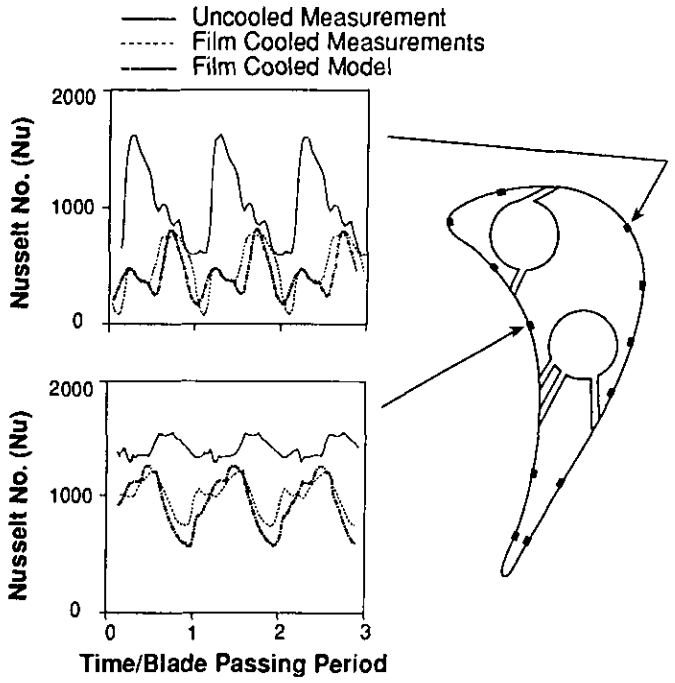

Fig. 14: A comparison of film-cooled measurements and predictions made with a simple, unsteady blowing model

Figure 14 compares the results of this calculation to the measured rotor film-cooled heat transfer and shows excellent agreement on both the pressure and suction surfaces. This agreement implies that film cooling at these locations is strongly influenced by unsteady blowing and that the above model captures the important physical features of the process. This result explains the apparent phase shift between the cooled and uncooled measurements as simply an artifact introduced by the unsteady blowing coupled to the propagation delay in the boundary layer. Additionally, the agreement between the model and data indicates that the boundary layer behavior is quasi-steady here and that film cooling performance can be successfully estimated in some cases without requiring film cooled, unsteady, multi-blade row codes (a great increase in complexity over the current state of the art).

The design of film cooled turbines is presently done assuming steady flow. We can take the time-averaged static pressure distribution as presented in Fig. 12 and calculate the resulting blowing and heat transfer (which is the design intent). Compared to the results of the unsteady model and measurements (which agree), the steady state predicted heat transfer is 12% too high on the suction surface and 5% too low on pressure surface. Thus, the unsteady blowing can impact the mean blade heat transfer and may need to be accounted for in cooling design systems. The unsteadiness driving the process is larger for highly loaded transonic turbines than for subsonic designs, so we would expect this effect to be somewhat exaggerated here compared to more lightly loaded designs.

SUMMARY AND CONCLUSIONS

The time-resolved heat transfer has been measured on the rotor of a fully cooled transonic turbine stage and compared with data from the same geometry operated in an uncooled configuration. The data show a considerable reduction in the average suction surface heat transfer with cooling but relatively little on the pressure surface. High blowing ratios were shown to provide much less effective cooling than lower ones. The results are similar over the center 3/4 of the span measured, implying that the flow in this region is mainly two-dimensional.

Comparisons were also made with cooled cascade measurements of the same profile. The rotor heat transfer on the suction surface was considerably less than that in the cascade. The time-resolved data revealed that the cooling, when effective, both reduced the d.c. level of heat transfer and changed the shape of the unsteady wave form. The principal unsteady driver for the film cooling was shown to be the unsteady rotor blade surface pressure distribution caused by blade row interactions. These modulate the cooling flow over a wide range which in turn generates fluctuations in cooling and heat transfer. A simple, linear model was shown to do a good job at predicting this effect. The unsteadiness resulted in a 12% heat transfer decrease at the suction surface location investigated, and a 5% increase on the pressure surface.

ACKNOWLEDGEMENTS

The authors would like to thank Dr. G.R. Guenette, Mr. C.W. Haldeman, and Dr. R.J.G. Norton for their generous assistance and stimulating comments, and Ms. D. Park for preparing the manuscript and figures. This work was supported by the Wright Laboratories, USAF, Dr. C. McArthur, program monitor, and Rolls-Royce Inc., Dr. R.J.G. Norton, technical monitor.

REFERENCES

Abhari, R.S., 1991, "An Experimental Study of the Unsteady Heat Transfer Process in a Film Cooled Fully Scaled Transonic Turbine Stage," Ph.D. Dissertation, Massachusetts Institute of Technology.

Abhari, R.S., Guenette, G.R., Epstein, A.H., Giles, M.B., 1991, "Comparison of Time-Resolved Measurements and Numerical Calculations," ASME 91-GT-268.

Ashley, H. and Landahl, M., 1965, *Aerodynamics of Wings and Bodies*, Addison-Wesley.

Ashworth, D.A., 1987, "Unsteady Aerodynamics and Heat Transfer Processes in a Transonic Turbine Stage," D. Phil. Thesis, Oxford University.

Dring, R.P., Blair, M.F. and Joslyn, H.D., 1980, "An Experimental Investigation of Film Cooling on a Turbine Rotor Blade," *ASME Journal of Engineering for Power*, Vol 102, pp 81-87.

Dunn, M.G., 1986, "Heat-Flux Measurements for the Rotor of a Full-Stage Turbine: Part I - Time-Averaged Results," ASME 86-GT-77.

Epstein, A.H., Guenette, G.R., Norton, R.J.G., Yuzhang, C., 1986, "High Frequency Response Heat Flux Gauge," *Review of Scientific Instruments*, Vol. 75, No. 4, pp. 639-649.

Giles, M.B., 1988, "UNSFLO: A Numerical Method for Unsteady Inviscid Flow in Turbomachinery," MIT Gas Turbine Laboratory Report No. 195.

Giles, M.B., Haimes, R., 1991, "Validation of a Numerical Method for Unsteady Flow Calculations," presented at ASME Gas Turbine Conference, Orlando, FL.

Goldstein, R.J. and Haji-Sheik, A., 1967, Japan Society of Mechanical Engineering, *1967 Semi-International Symposium*, pp 213-218, Tokyo.

Goldstein, R.J., Eckert, E.R.G. and Burggraf, F., 1974, "Effect of Hole Geometry and Density on Three-Dimensional Film Cooling," *International Journal of Heat and Mass Transfer*, Vol. 17, pp. 595-607.

Goldstein, R.J. and Chen, H.P., 1985, "Film Cooling on a Gas Turbine Blade Near the End Wall," *ASME J. of Eng. for Gas Turbine and Power*, Vol. 107, pp. 117-122.

Guenette, G.R., Epstein, A.H., Giles, M.B., Haimes, R. and Norton, R.J.G., 1989, "Fully Scaled Transonic Turbine Rotor Heat Transfer Measurements," *Journal of Turbomachinery*, Vol. 111, pp. 1-7.

Ito, S., Goldstein, R.J., Eckert, E.R.G., 1978, "Film Cooling of a Gas Turbine," *ASME Journal of Engineering for Power*, Vol. 100, pp. 476-481.

Norton, R.J.G., 1987, Private Communications, Rolls Royce Inc.

Rigby, M.J., Johnson, A.B., Oldfield, M.L.G., 1990, "Gas Turbine Rotor Blade Film Cooling With and Without Simulated NGV Shock Waves and Wakes," ASME 90-GT-78.

Schwarz, S.G. and Goldstein, R.J., 1988, "The Two-Dimensional Behavior of Film Cooling Jets on Concave Surfaces," ASME 88-GT-161.

Takeishi, K., Aoki, S., Sato, T., Tsukagoshi, K., 1991, "Film Cooling on a Gas Turbine Rotor Blade," ASME 91-GT-279.

Whitten, D.G., Moffat, R.J. and Kays, W.M., 1970, "Heat Transfer to a Turbulent Boundary Layer With Non-Uniform Blowing and Surface Temperature," 4th International Heat Transfer Conference, Paris-Versailles.